

# REPLAY OF THE 2011 MW 9.0 GREAT EAST JAPAN EARTHQUAKE IN SIMULATED REAL-TIME MODE WITH INTEGRATED 1 HZ GPS AND 100 HZ ACCELEROMETER DATA FOR RAPID SOURCE CHARACTERIZATION, EARTHQUAKE RESPONSE SPECTRA AND TSUNAMI PREDICTION

Yehuda BOCK<sup>1</sup>, Diego MELGAR<sup>1</sup>, Brendan W. CROWELL<sup>1</sup>, Dominga SANCHEZ<sup>2</sup>,  
and José RESTREPO<sup>2</sup>

<sup>1</sup> Research Geodesist, Institute of Geophysics and Planetary Physics, Scripps Institution of Oceanography, La Jolla, CA, USA, ybock@ucsd.edu

<sup>2</sup> Professor, Department of Structural Engineering, University of California San Diego  
La Jolla, CA, USA, jrestrepo@ucsd.edu

**ABSTRACT:** We replay real-time data from 190 1 Hz GEONET GPS and 100 Hz NIED accelerometer stations that are within 1-2 km of each other in the region of ground deformation during the 2011 Mw 9.0 Great East Japan earthquake. Using an on-the-fly Kalman filter/smoothing, we estimate three-dimensional 100 Hz broadband (static and dynamic) displacements with mm precision. Using the displacements, we derive a finite fault slip model and earthquake response spectra, which are achievable within 3-4 minutes of earthquake initiation. We discuss implications for rapid tsunami warning.

**Key Words:** Great East Japan earthquake, GPS/seismic integration, earthquake characterization, response spectra, tsunami warning

## INTRODUCTION

Responses to recent great earthquakes and ensuing tsunamis in Sumatra, Chile and Japan with the resulting loss of life and damage to infrastructure demonstrate that our ability to evaluate the magnitude and source of catastrophic earthquakes and their tsunamigenic potential in the first seconds to minutes after the initiation of rupture, even with modern seismic instrumentation, is problematic. High-gain, broadband seismometers, which easily record long-period motion required for rapid modeling, clip when shaking is too intense, i.e. when located close to the source of large earthquakes. Secondly, low-gain, strong motion accelerometers, which are specifically designed to be capable of recording intense ground motions, cannot record long-period data. During strong shaking accelerometers are rotated in addition to being translated and not capable of discerning between these two different kinds of motions (*Graizer, 1979; Iwan et al., 1985*); hence, rotations are recorded as translations. These spurious translations produce what is commonly known as baseline offsets (*Boore et al., 2002*), which make it problematic to extract all of the long-period information in the seismic

record. Post-processing schemes exist that can extract long-period information from strong motion data (Boore and Bommer, 2005); however, these correction schemes are subjective and multiple correction schemes yield seemingly plausible waveforms without an objective criterion to decide which one is the correct one, certainly not in real time (Boore et al., 2002). Most importantly, the static (permanent) deformation is lost.

Earthquake early warning (EEW) systems, first developed in Japan, have now been implemented or are under development in several countries (e.g., Gasparini et al., 2007, Allen et al., 2009a,b; Astiz, 2009). However, they currently rely exclusively on seismic data and methods (including in Japan) with the above mentioned limitations. By being insensitive to finite fault slip, seismic-based EEW systems are unable to distinguish between a magnitude 6.5 event from a much larger event as was evident during the 2011 Mw 9.0 Great East Japan earthquake. A good summary of the existing EEW algorithms and their limitations are given by Allen et al. (2009b). The ability of *P*-wave-based methods to rapidly and accurately detect large earthquakes ( $M > 7$ ) is controversial (Allen et al., 2009b) and this is where broadband displacements from GPS or GPS/seismic integration as shown in this paper can play a major role. We have shown for the 2003 Mw 8.3 Tokachi-oki earthquake in Japan and the 2010 Mw 7.2 El Mayor-Cucapah earthquake in northern Baja California, Mexico that a fast centroid moment tensor (CMT) solution (Melgar et al., 2011) and a full finite fault slip model (Crowell et al., 2012) can be estimated within 2-3 minutes of those events using near-source GPS networks. In addition, scaling relationships derived from displacement measurements from several large earthquakes with near-field GPS/seismic network monitoring can be applied directly to EEW algorithms (Crowell et al., 2009).

Structural monitoring is also currently limited to seismic instrumentation, in particular accelerometers, and suffers the same limitations. Real time monitoring of buildings and infrastructure is contemplated more and more as a desirable asset by the engineering community (Celebi et al., 2004; Masri et al. 2004; Ko and Ni, 2005) for a number of reasons. The benefits of full-bandwidth displacement waveforms during strong shaking as well as during quiescent periods are obvious. Real-time monitoring serves an academic purpose in that it permits comparison between the actual and theoretical responses of a structure and it allows engineers to explain and model the observed damage product of a particular excitation. It also serves a very practical purpose in that it permits rapid assessment of building conditions following an event and allows inspectors to rely on data and not just visual inspections to tag a building green, yellow or red. This directly impacts the rapidity and accuracy of inspections. Additionally, real-time monitoring serves engineering purposes on multiple time scales. Immediately after an event it helps to assess the state of a structure, but in the mid to long-term sense it allows structural engineers to assess performance-based design and analysis procedures, and perform state-of-health monitoring and long-term damage detection.

Earthquake early warning, source imaging and structural monitoring, hence, are limited in terms of the size of the earthquake that can be evaluated in real time. Another example is regional waveform matching techniques that invert for the moment tensor (MT, Dreger and Helmberger, 1990; Dreger 2003). One notable exception is the W-phase algorithm. This represented an important advance in computing centroid moment tensors (CMTs) as quickly as possible for large events. The W phase algorithm was developed by Kanamori and Rivera (2008), who elaborated on Kanamori's (1993) observation of the W phase, a long-period phase arriving in between the direct *P* and *S* waves. They showed that inversion for the MT using data as close as 15° from the source is viable. W phase inversion algorithms currently run in real time at the USGS, Pacific Tsunami Warning Center (PTWC) and Institut du Physique du Globe de Strasbourg (IPGP-EOST, Hayes et al. 2009). Since the W phase arrives well before large amplitude surface waves and remains on-scale far longer such inversion algorithms have shown to be a marked improvement in rapid computation of CMT solutions for large events over traditional waveform matching techniques. W phase-based inversion schemes, while very robust, require long-period displacement records, e.g. 200–1000 s for the 2011 Great East Japan event (Duputel et al. 2011). These are almost always unusable in real time close to the source for the reasons discussed above; velocity instruments clip and it is difficult to extract long period motions from strong-motion accelerometer data because of tilts and rotations of the instruments (Boore and Bommer, 2005).

For the Great East Japan event it took 20 min after origin time to arrive at the first CMT solutions by

agencies running W phase algorithms (*Duputel et al.* 2011), even though the rupture had a duration of 2 minutes (*Simons et al.* 2011). This delay was due to the reliance on teleseismic data. After several iterations using progressively more data, the final CMT solution was obtained by the National Earthquake Information Centre (NEIC) 90 minutes after origin time using data up to 90° from the rupture. The first estimate of moment magnitude was obtained in about 3 min by the Japan Meteorological Agency (JMA), but was grossly underestimated at  $M_w = 6.8$ . *Duputel et al.* (2011) documented that in the numerous iterations between agencies the nodal planes were somewhat consistent with only minor variations in strike dip and rake, the magnitudes oscillated between  $M_w$  8.8 and 9.0 after the 20-minute mark, but the centroid locations varied by as much as 2° and 60 km in depth. These solutions are robust enough and fast enough for ocean basin-wide tsunami early warning, and in this regard the W phase algorithm is a resounding success. Numerous tsunami warnings for large earthquakes (<http://ptwc.weather.gov/>) issued by the PTWC attest to this. Nonetheless, issuing a robust early warning in the near source region remains elusive. Only Japan has such a system in place, there is no near-field early warning system anywhere else in the world. However, due to the Great East Japan earthquake's magnitude being severely underestimated the initial tsunami warnings issued by JMA were a poor assessment of the actual intensity of the tsunami (*Ozaki*, 2011) because the fundamental problem of determining an earthquake's dimension with local and regional data in real-time remains only partially solved. In an attempt to extend the W phase algorithm and incorporate local data *Rivera et al.* (2011) concluded that data closer than 3° to the source is unusable because the point source assumption in the W phase algorithm can no longer be used to model the event.

## INTEGRATION OF GPS AND SEISMIC DATA

Japan has the world's most advanced earthquake early warning system and the only early tsunami warning capability in near-source coastal regions. However, the effectiveness of the Japanese response to the 2011  $M_w$  9.0 Great East Japan earthquake was certainly diminished by strict reliance on traditional seismic methods to estimate earthquake magnitude and ground shaking, while failing to build into their impressive earthquake early warning system the availability of real-time 1 Hz data from the 1200-station GPS network (GEONET – *Miyazaki et al.*, 1998). If real-time displacements from GPS and accelerometer data had been available an accurate estimate of moment magnitude could have been obtained very soon after the rupture ended, an order of magnitude improvement in latency compared to traditional seismic methods. This was critical for tsunami warning since the first waves hit the coastline after only 30 minutes.

Permanent deformation is the best source of long-period information about an earthquake. GPS is well equipped to measure permanent deformation and thus to characterize an earthquake as first demonstrated for magnitude estimation of the 1992  $M_w$  7.3 Landers earthquake in southern California (*Blewitt et al.* 1993; *Bock et al.* 1993). There have been some attempts to address the use of GPS static deformation estimates in rapid source models, notably by *Blewitt et al.* (2006) who showed that given an epicentral location and assuming thrust faulting for the 2004  $M_w$  9.2 Sumatra–Andaman earthquake, one could have estimated an accurate magnitude within 15 min of the origin time using global GPS stations at regional to teleseismic distances. In *Bock et al.* (2011), building on numerical simulations by *Smyth and Wu* (2006) and applied to bridge monitoring by *Kogan et al.* (2008), we demonstrated that traditional seismological time series can be combined with GPS time series to produce data products of superior precision in real time.

In Figure 1a, we show the entire period of seismic shaking at collocated GPS and accelerometer data at P494/WES in the vertical component during the 2010  $M_w$  7.2 El Mayor-Cucapah earthquake in northern Baja California. This earthquake was recorded by real-time GPS and accelerometer instruments throughout southern California, which was affected by significant crustal deformation. The observed broadband velocities clipped even before the arrival of the S-wave at the station, while the Kalman-filtered estimated velocity waveforms record the entire event at the 100 Hz rate of the accelerometer. In Figure 1b, we show the first 12 s of the vertical broadband velocity record at WES after the Southern California Earthquake Center's P-wave pick and overlay the

Kalman-filter-estimated velocities. That the broadband seismic data and the waveform estimated by Kalman smoothing are indistinguishable is striking, given also that the GPS resolution is poorest in the vertical direction. In Figure 1c, we compare displacements derived by (single) integration of the 12 s seismometer record at WES, and the 100 Hz smoothed Kalman filter full spectrum displacements. It is clear that we can detect the small-amplitude P-wave recordings with a precision and accuracy of about 1 mm. This is a significant improvement over the 1 Hz GPS-only solutions where the vertical precision is on the order of several cm, precluding P-wave detection. Figure 3c also shows the poor results obtained by on-the-fly double integration of the accelerometer data. We obtained better results in post processing with baseline corrections and function fitting procedures (*Boore et al., 2002*). Although the dynamic motions could be extracted, the static displacements were lost. With the addition of GPS displacements, the double integration can be performed on-the-fly using only raw accelerometer records. The Kalman filtered records capture both the shaking and the permanent deformation, effectively recording the full bandwidth of seismic motion and allowing for the recording of near-source deformation during large earthquakes.

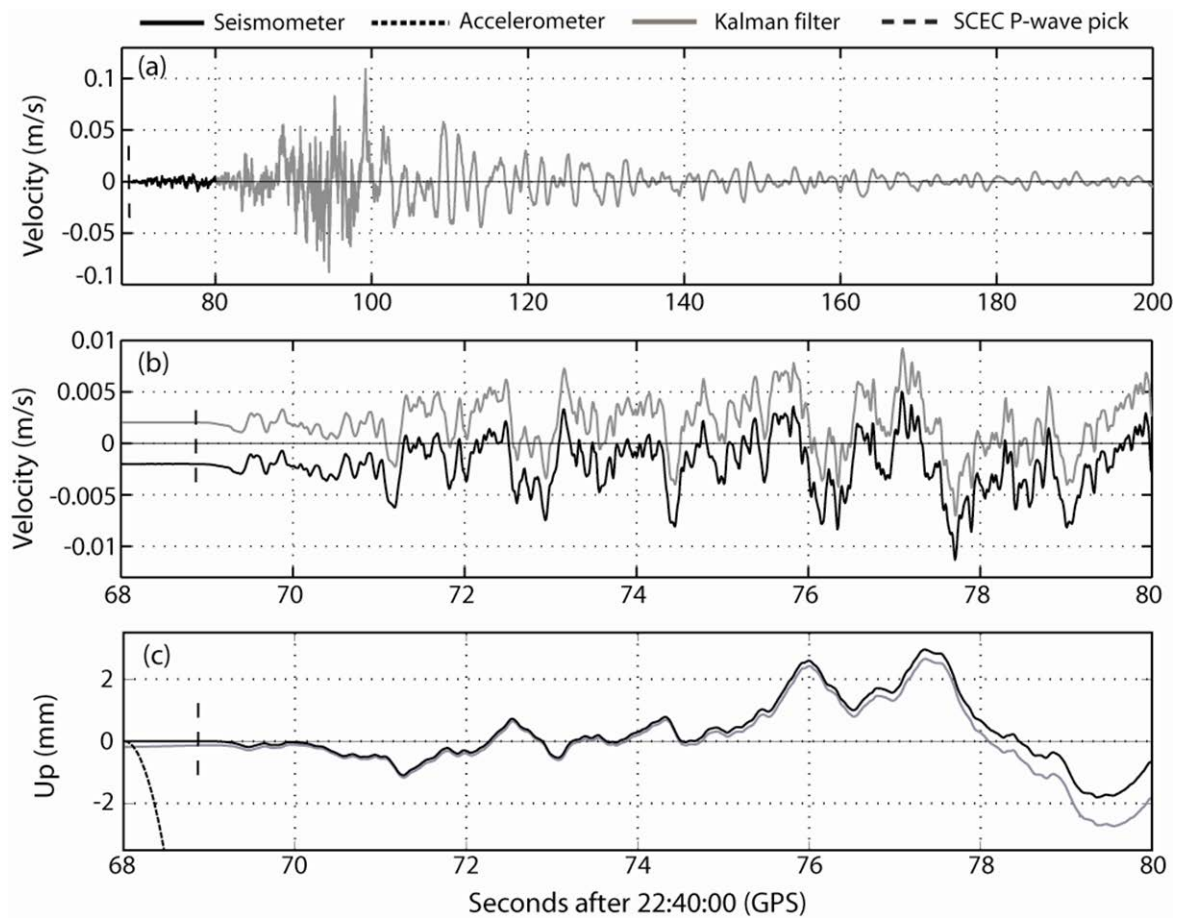


Figure 1. Combining GPS and accelerometer data into a single stream creates a low-gain broadband seismometer that never clips. Adapted from *Bock et al. (2011)*.

## BROADBAND DISPLACEMENTS FOR THE GREAT EAST JAPAN EARTHQUAKE

For the Great East Japan earthquake, we analyzed in simulated real-time mode 1 Hz GPS (RINEX) data from over 1000 GEONET stations (*Miyazaki et al., 1998*) in 30 prefectures on Honshu

and Hokkaido islands (Figure 2) using the method of instantaneous positioning (*Bock et al., 2000; Bock et al., 2011*). Three-dimensional 1 Hz relative displacements were estimated in triangular subnetworks derived from a Delaunay triangulation of all stations. We used the International Reference Frame (ITRF) 2005 coordinates obtained from the ARIA group at Caltech/JPL (*Simons et al., 2011*) as *a priori* values for analysis of the triangular subnetworks. Using the coordinates of GPS station 0848 on the northern tip of Hokkaido island as fixed, we computed three-dimensional displacements of all other stations using a network adjustment procedure described in *Crowell et al. (2009)*. We then searched for NIED KiK-net and K-Net accelerometer stations (*Aoi et al., 2004*) that were within 1-2 km of a GEONET GPS station. We identified 190 “collocated” stations in the region of deformation, all with 100 Hz accelerometer data which had been triggered by the earthquake. The two data types, 1 Hz GPS displacements and 100 Hz accelerometer data, were analyzed in real-time mode using a Kalman smoother as described in *Bock et al. (2011)*, resulting in 100 Hz displacements for all 190 collocated stations. As is typical with GPS data analysis, the 1 Hz GPS-only displacements have a precision of about 1 cm in the horizontal directions and 5 cm in the vertical direction. Combining the GPS displacements with the much more precise accelerometer data, results in 100 Hz broadband displacements with a precision of at least 1 mm in all three components (see also Figure 1) and an accurate representation of the dynamic shaking and the evolution of the permanent deformation throughout the network.

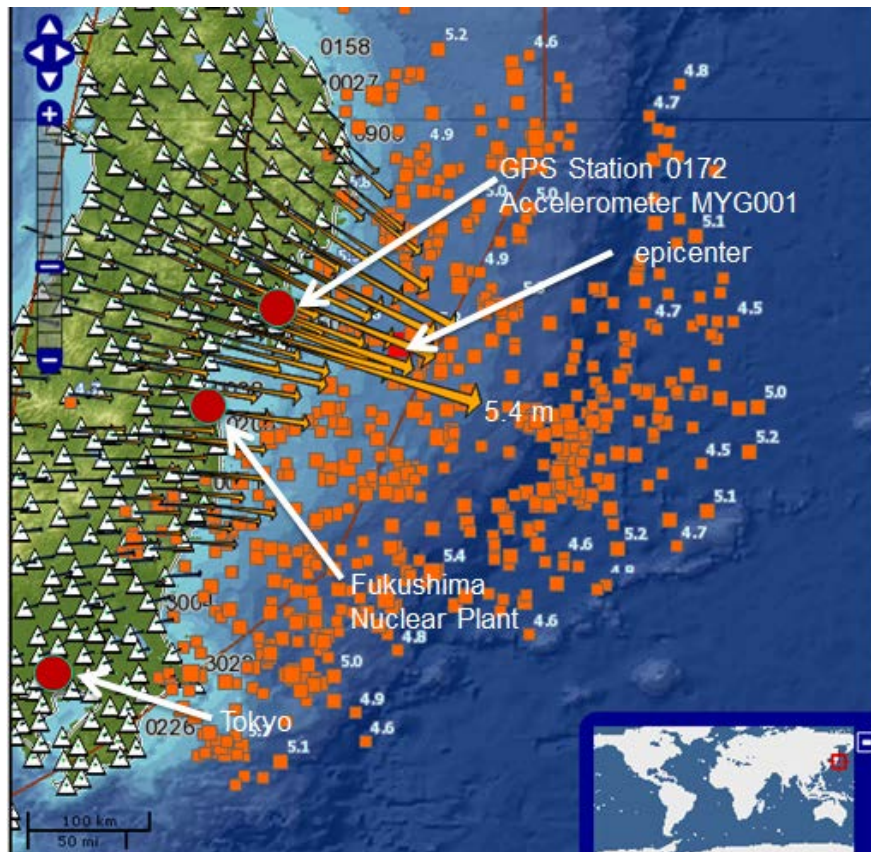


Figure 2. Coseismic displacements in the epicentral region computed from Japan’s 1200+ station CGPS Network (GEONET) by ARIA group at Caltech/JPL (courtesy of Susan Owen, JPL). Maximum surface displacement on land was 5.24 meters at station 0550 on coast.

In Figure 3, we show the 100 Hz displacement record for the instruments (collocated 1 Hz GPS receiver 0172 and 100 Hz strong-motion accelerometer MYG001) on the coast across from the earthquake’s epicenter (Figure 2) estimated in simulated real-time mode with the Kalman filter



## RESPONSE SPECTRA FROM BROADBAND DISPLACEMENTS

Traditionally earthquake response spectra have been computed from measured ground accelerations (e.g., *Celebi et al.* 2004; *Celebi* 2006) for two reasons: (1) strong ground motions are recorded only on acceleration sensors because velocity sensors clip and displacement measurements have been thus far unavailable, and (2) accelerations are forces per unit mass and thus can be directly related to loading of a structure and hence are a suitable description of an single degree of freedom (SDF) oscillator. Using the displacements waveforms estimated at the 190 collocated GPS/accelerometer stations for the Great East Japan earthquake, we computed response spectra for each station by solving the ordinary differential equation for a SDF oscillator using a finite difference scheme for three different forcing functions: (1) the raw 100 Hz accelerometer data, (2) the raw 1 Hz GPS displacements, and (3) the 100 Hz Kalman-filtered GPS/accelerometer combination.

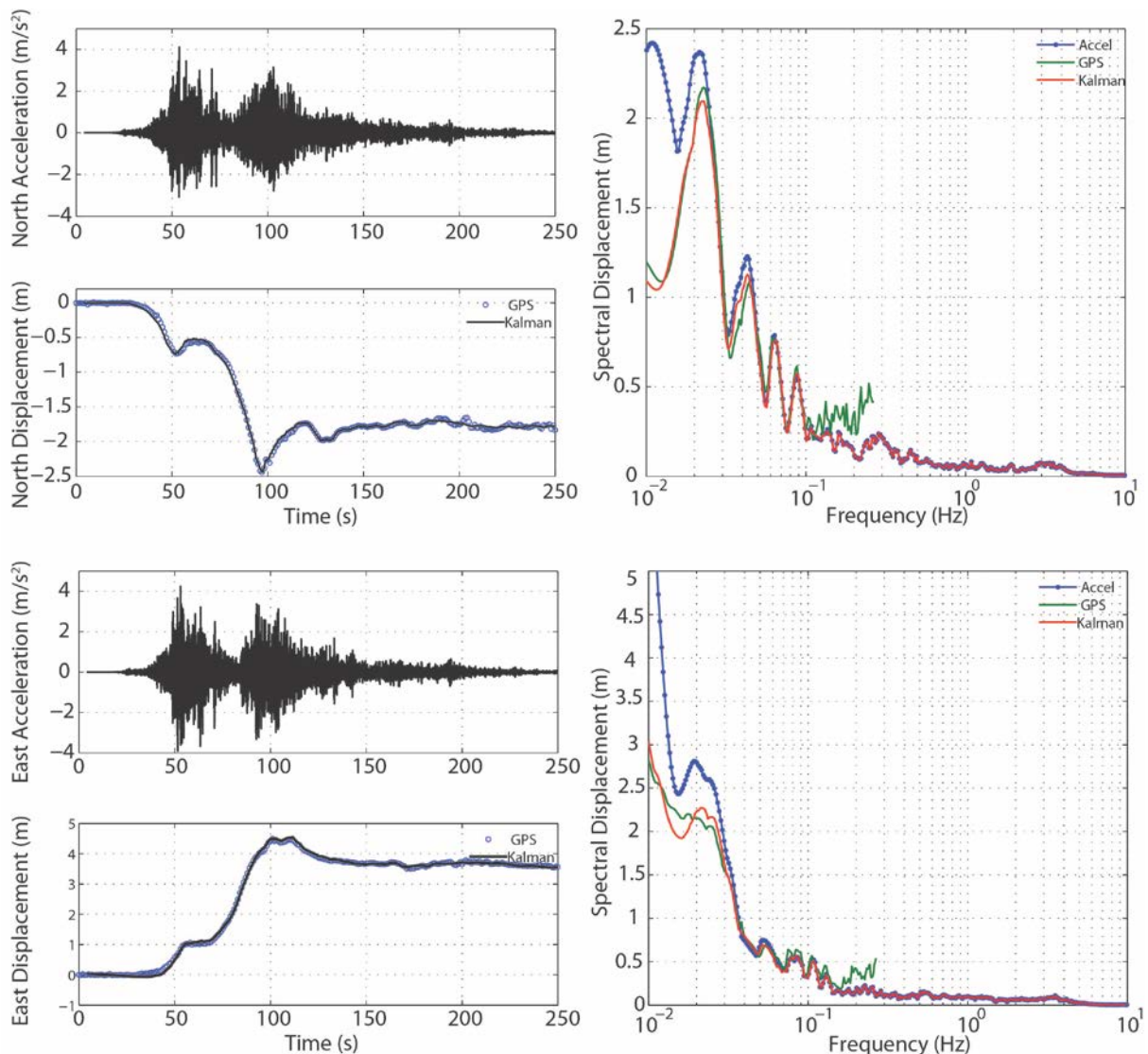


Figure 4. Response spectra displacements for collocated GPS station 0172 and accelerometer station MYG001 in north and east directions obtained by solving the ordinary differential equation for a SDF oscillator with a finite difference scheme. Shown are spectra for three forcing functions: (1) the raw 100 Hz accelerometer data, (2) the raw 1 Hz GPS displacements, and (3) the 100 Hz Kalman-filtered GPS/accelerometer combination.

Figure 4 shows a typical example for the integration of displacement data (Figure 3) from GPS station 0172 and accelerometer station MYG001 (Figure 2). The noise levels in the displacement time series are significantly reduced with the GPS/accelerometer combination and we capture both high-frequency shaking as well as the final coseismic (static) offsets. The spectra display some interesting characteristics. Because of limited sampling frequency, the GPS spectra are limited to frequencies smaller than 0.5 Hz. Additionally, we routinely observe that in the frequency range between 0.1 and 0.5 Hz the GPS data lead to a small over-estimation of the spectral displacement when compared to the accelerometer spectra, which may be explained by aliasing of signals outside the Nyquist frequency. Conversely, at lower frequencies the accelerometer spectra are significantly larger (1 m in the east component and 2.5 m in the north component) than the ones estimated from the GPS data alone. As we expect, the GPS spectra seem to better capture the spectral response at these long periods while the accelerometer spectra do a better job at the high frequencies. However, the spectral estimates from the GPS/accelerometer combination coincide with the GPS spectra at low frequencies and with the accelerometer spectra at high frequencies. Thus, with a single data product one can obtain the full spectrum of information.

As *Celebi and Sanli* (2002) point out, in addition to monitoring free-field displacements, the capacity to directly measure displacements on structures directly impacts real-time monitoring capacity. For example, the analysis techniques discussed for the 1994 Mw 6.7 Northridge earthquake by *Darragh et al.* (1994) involve bandpass filtering of the strong-motion records, usually in the 0.2-25 Hz range. This might be unsuitable for monitoring when long-period information is desired; even so, monitoring of large structures is still performed with accelerometer-only instrument packages (e.g., *Ventura et al.*, 2003) mainly because alternate methodologies have not yet been proven to be practical. Examples of GPS-only based monitoring exist (*Lovse et al.* 1995; *Stein et al.* 1997; *Hudnut and Behr*, 1998) but the technology has stagnated in this regard. Deployment of GPS for monitoring following the proposal of *Celebi and Sanli* (2002) has been rather limited. However, the optimal combination of GPS and accelerometer data described here along with lower costs for both types of sensors should expand the use of this technology for monitoring structures.

## RAPID SOURCE CHARACTERIZATION AND TSUNAMI WARNING

From the broadband displacement waveforms, we leveraged the improved accuracy (especially in the vertical) to develop a coseismic model of the earthquake 200 seconds after initiation (Figure 5). We followed the methods of *Crowell et al.* [2012] to rapidly model the event, whereby we utilized Green's functions from *Okada* [1985], a first-order Tikhonov regularization with a generalized smoothness parameter, and a moving average window of 50 seconds on the displacement waveforms. We used the Slab 1.0 model [*Hayes and Wald*, 2009; *Hayes et al.*, 2009] of the Kuril-Japan trench as the fault interface. Results from our model show that there is a large displacement from the trench towards the hypocenter, with some smaller-scale features towards the south. The solution computed here is obtainable within less than 4 minutes of the event, which would have proved invaluable to tsunami warning and emergency first responders.

Given the finite fault slip model (Figure 5) the next step is to incorporate numerical modeling algorithms to rapidly predict expected tsunami intensity parameters such as maximum amplitude, inundation distance and run-up height in the near-source region. *Ohta et al.* (2012) have taken a similar approach but their algorithm is limited in one important way. It assumes that the fault is a rectangle that slips coherently, that is, slip is the same everywhere on that fault plane. As we know from *Simons et al.* (2011) and from our rapid modeling, slip on the Great East Japan earthquake fault is highly heterogeneous; it has considerable amounts of slip trenchward, possibly explaining the anomalous tsunami intensity. Thus, assuming homogenous slip could lead to severe mis-modeling of the expected tsunami.

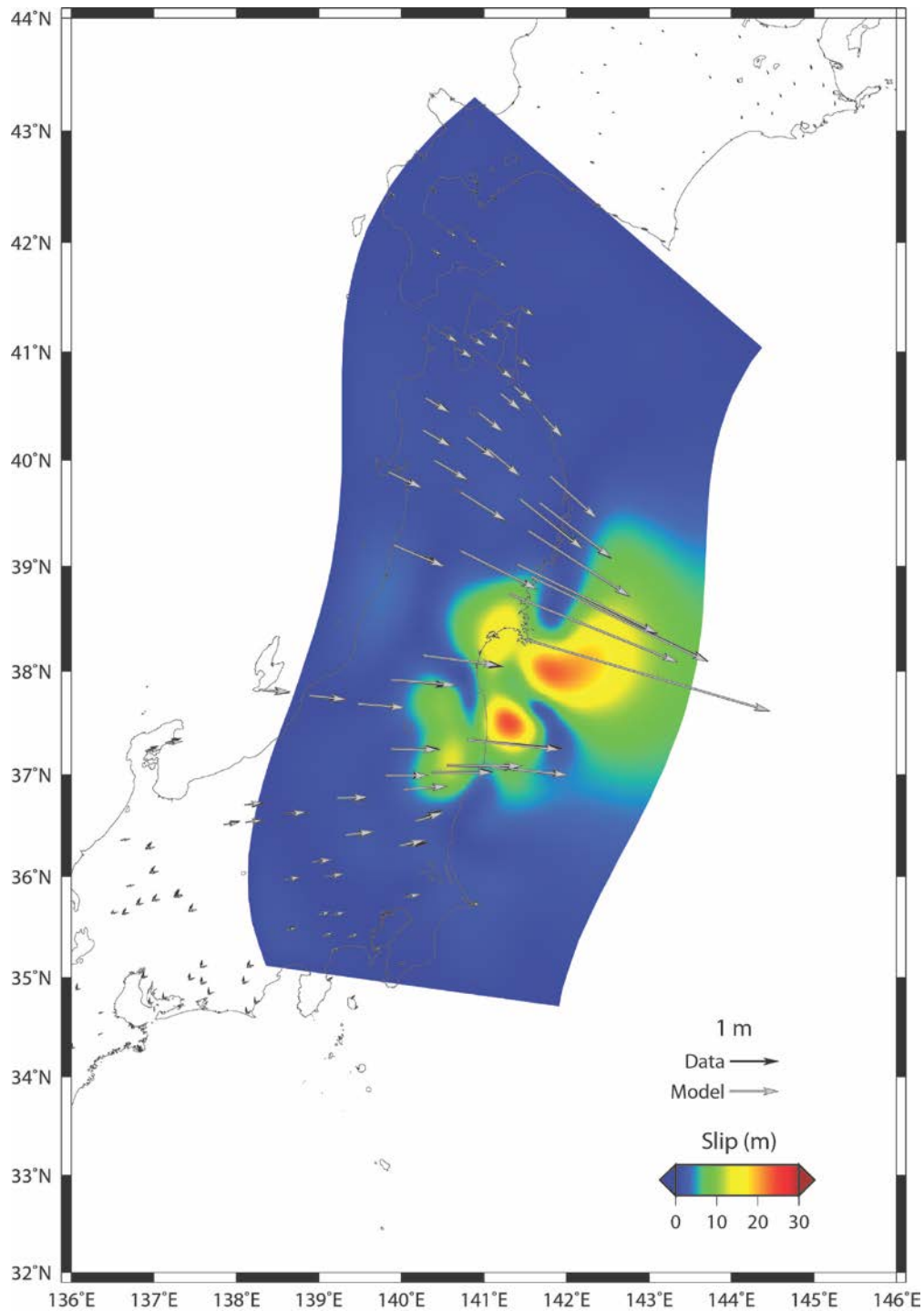


Figure 5. Finite fault-slip model for the March 11, 2011 Mw 9.0 Great East Japan earthquake estimated in simulated real-time mode based on the 100 Hz displacements for the 190 GPS/accelerometer stations. The slip (in meters) denoted by the color scale is valid for 200 seconds after earthquake and denotes primarily the coseismic motion. The moment magnitude is estimated to be 8.95. The gray arrows denote the observed (horizontal) displacements and the black arrows are the model displacements. The rms of fit is 152 mm.

## CONCLUSIONS

Existing seismic methods are limited in the near-field for rapid response after large earthquakes. For the Great East Japan earthquake, it took about 20 minutes to determine that a great earthquake was occurring. We have shown that using the existing GPS and accelerometer networks in Japan, characterization of the earthquake, including magnitude and finite fault slip, could have completed within less than 4 minutes of initiation. These results could have had important implications for rapid structural damage assessments and early warning for the ensuing devastating tsunami.

## ACKNOWLEDGMENTS

We thank Japan's GSI for GEONET 1 Hz data and NIED for 100 Hz KiK-net and K-Net accelerometer data for the 2011 Great East Japan earthquake. This paper was funded by NASA/AIST Grant No. NNX09AI67G.

## REFERENCES

- Allen, R. M., Gasparini, P., and Kamigaichi, O., eds. (2009a). "New methods and applications of earthquake early warning." *Geophys. Res. Lett.* 36, L00B05, L00B08, L00B03, L00B04, L00B02, L00B06, L00B01, L00B07.
- Allen, R.M., Gasparini, P., Kamigaichi, O., and Bose, M. (2009b). "The Status of Earthquake Early Warning around the World: An Introductory Overview," *Seismo. Res. Lett.*, 80(5) p682-693, doi: 10.1785/gssrl.80.5.682.
- Astiz, L., ed. (2009). "Special issue on earthquake early warning," *Seismo. Res. Lett.*, 80(5).
- Blewitt, G., Heflin, M.B., Hurst, K.J., Jefferson, D.C., Webb, F.H. and Zumberge, J.F. (1993). "Absolute far-field displacements from the 28 June 1992 Landers earthquake sequence," *Nature*, **361**, 340–342.
- Blewitt, G., Kreemer, C., Hammond, W.C., Plag, H.P. and Stein, S. (2006). "Rapid determination of earthquake magnitude using GPS for tsunami warning systems," *Geophys. Res. Lett.*, **33**, doi:10.1029/2006GL026145.
- Bock Y., et al. (1993), "Detection of crustal deformation from the Landers earthquake sequence using continuous geodetic measurements," *Nature*, 361, 337-340.
- Bock, Y., Nikolaidis, R., de Jonge, P. J. and Bevis, M. (2000), "Instantaneous geodetic positioning at medium distances with the Global Positioning System," *J. Geophys. Res.*, 105, 28,223-28,254.
- Bock, Y., Melgar, D. and Crowell, B.W. (2011). "Real-time strong-motion broadband displacements from collocated GPS and accelerometers," *Bull. Seism. Soc. Am.*, 101, 2904-2925.
- Boore, D.M., Stephens, C.D. and Joyner, W.B. (2002). "Comments on Baseline Correction of Digital Strong-Motion Data: Examples from the 1999 Hector Mine, California, Earthquake," *Bull. Seism. Soc. Am.*, 92(4), 1543-1560.
- Boore, D.M. and Bommer, J.J. (2005). "Processing of strong-motion accelerograms: needs, options and consequences," *Soil Dyn. Earthq. Eng.*, 25, 93-115
- Celebi, M. and Sanli, A. (2002). "GPS in Pioneering Dynamic Monitoring of Long-Period Structures," *Earthquake Spectra*, 18(1), 47-61.
- Celebi, M., Sanli, A., Sinclair, M., Gallant, S. and Radulescu, D. (2004). "Real-Time Seismic Monitoring Needs of a Building Owner – and the Solution: A Cooperative Effort," *Earthquake Spectra*, 20(2), 333-346.
- Celebi, M. (2006). "Real-Time Seismic Monitoring of the New Cape Girardeau Bridge and Preliminary Analyses of Recorded Data: An Overview," *Earthquake Spectra*, 22(3), 609-630.
- Crowell, B., Bock, Y. and Squibb, M. (2009). "Demonstration of earthquake early warning using total displacement waveforms from real time GPS networks," *Seismo. Res. Lett.*, 80(5), 772-782, doi:

10.1785/gssrl.80.5.772.

- Crowell, B., Bock, Y., and Melgar, D (2012), Real-time inversion of GPS data for finite fault modeling and rapid hazard assessment, *Geophys. Res. Lett.*, in revision.
- Darragh, R., Cao, T., Graizer, V., Shakal, A. and Huan, M. (1994). "Los Angeles Code-Instrumented Building Records from the Northridge, California Earthquake of January 17 1994: Processed Release No. 1," California Strong Motion Instrumentation Program, 132pp.
- Duputel, Z., Rivera, L., Kanamori, K., Hayes, G.P., Hirsorn, B. and Weinstein, S. (2011). "Real-time W phase inversion during the 2011 Great East Japan earthquake," *Earth Planets Space*, 63(7), 535-539.
- Gasparini, P., Manfredi, G. and Zschau, J. (Eds) (2007). "Earthquake Early Warning Systems," Springer, ISBN-13 978-3-540-72240-3.
- Graizer, V. M. (1979). "Determination of the true ground displacement by using strong motion records," *Izv. Phys. Solid Earth* **15** 875-885.
- Hayes, G.P. and Wald, D.J. (2009). "Developing framework to constrain the geometry of the seismic rupture plane on subduction interfaces a priori: a probabilistic approach," *Geophys. J. Int.*, **176**, 951–964.
- Hayes, G.P., Rivera, L. and Kanamori, H. (2009). "Source inversion of the W phase: real-time implementation and extension to low magnitudes," *Seism. Res. Lett.*, **80**(5), 817–822.
- Hudnut, K. W., and Behr, J.A. (1998). "Continuous GPS monitoring of structural deformation at Pacoima Dam, California," *Seismol. Res. Lett.*, 69, 299–308.
- Ide, S., et al. (2011). "Shallow Dynamic Overshoot and Energetic Deep Rupture in the 2011 Mw 9.0 Great East Japan Earthquake," *Science*, 32, doi: 10.1126/science.1207020 2011.
- Iwan, W. D., Mooser, M. A., and Peng, C. Y. (1985). "Some observations on strong motion earthquake measurements using a digital accelerograph," *Bull. Seism. Soc. Am.* **75** 1225-1246.
- Kanamori, H., (1993). "W-phase," *Geophys. Res. Lett.*, **20**(16), 1691–1694.
- Kanamori, H. and Rivera, L. (2008). "Source inversion of W phase: speeding up seismic tsunami warning," *Geophys. J. Int.*, **175**, 222–238.
- Ko, J. M. and Ni, Y.Q. (2005). "Technology developments in structural health monitoring of large scale bridges," *Engineering Structures*, 27(12), 1715-1725
- Kogan, M. G., Kim, W-Y., Bock, Y. and Smyth, A. W. (2008). "Load response on the Verrazano Narrows Bridge during the NYC Marathon revealed by GPS and accelerometers," *Seismo. Res. Lett.*, 79(1), 12-19.
- Lovse, J.W., Teskey, W.F., Lachapelle, G., and Cannon, M. E. (1995). "Dynamic deformation monitoring of a tall structure using GPS technology," *J. Surv. Eng.*, 121, 35-40.
- Masri, S. F., Sheng, L., Caffrey, J. P., Nigbor, R. L., Wahbeh, M. and Abdel-Ghaffar, A. M. (2004). "Application of a web-enabled real-time structural health monitoring system for civil infrastructure systems," *Journal of Smart Materials and Structures*, 13, 1269-1283.
- Melgar, D., Bock, Y. and Crowell, B.W., (2012). "Real-Time Centroid Moment Tensor Determination for Large Earthquakes from Local and Regional Displacement Records," *Geophys. J. Int.*, doi:10.1111/j.1365-246X.2011.05297.x.
- Miyazaki, S., Tsuji, H., Hatanaka, Y. and Tada, T. (1998). "The nationwide GPS array as an earth observation system," *Bull. Geogr. Surv. Inst.*, 44, 11-22.
- Ohta, Y., et al. (2011). "Quasi real-time fault model estimation for near-field tsunami forecasting based on RTK-GPS analysis: Application to the 2011 Great East Japan Earthquake (Mw 9.0)," *J. Geophys. Res.*, doi:10.1029/2011JB008750, in press.
- Okada, Y. (1985). "Surface deformation due to shear and tensile faults in a half-space," *Bull. Seism. Soc. Am.*, 75(4) 1135-1154.
- Ozaki, T. (2011). "Outline of the 2011 off the Pacific coast of Tohoku Earthquake (Mw 9.0) --Tsunami warnings/advisories and observations", *Earth Planets Space*, 63(7), 827-830.
- Rivera, L.A., Kanamori, H. and Duputel, Z. (2011). "W phase source inversion using the high-rate regional GPS data of the 2011 Great East Japan earthquake," *Presented at the 2011 AGU Fall Meeting*, Abstract G33C-04.
- Sato, M. et al. (2011). "Displacement above the Hypocenter of the 2011 Great East Japan Earthquake,"

- Science*, 32, doi:10.1126/science.1207401.
- Simons, M. *et al.* (2011). “The 2011 magnitude 9.0 Great East Japan earthquake: mosaicking the megathrust from seconds to centuries,” *Science*, **332**(6036), 1421–1425.
- Smyth, A. and Wu, M. (2006). “Multi-rate Kalman filtering for the data fusion of displacement and acceleration response measurements in dynamic system monitoring,” *Mechanical Systems and Signal Processing*, doi:10.1016/j.ymssp.2006.03.005.
- Stein, R.S., Hudnut, K. W., Satalich, J., and Hodgkinson, K. M. (1997). “Monitoring seismic damage to bridges and highways with GPS: Insights from the 1994 Northridge earthquake,” in *Proc. Natl. Seismic Conf. on Bridges and Highways*, Fed. Highway Admin. and Calif. Dept. of Transp., 347-360.
- Song, Y. T. (2007). “Detecting tsunami genesis and scales directly from coastal GPS stations,” *Geophys. Res. Lett.*, *34*, doi:10.1029/2007GL03168.
- Ventura C., Laverick, B., Brincker, R., and Andersen, P. (2003) “Comparison of dynamic characteristics of two instrumented tall buildings,” in 21st international modal analysis conference (IMAC), Copenhagen, Denmark, online memoirs.